




Decompositions of multiple controlled-Z gates on various qubit-coupling graphs

Ken M. Nakanishi ^{1,*}, Takahiko Satoh ^{2,3,†} and Synge Todo ^{1,4,5,‡}

¹*Institute for Physics of Intelligence, The University of Tokyo, Tokyo 113-0033, Japan*

²*Quantum Computing Center, Keio University, Yokohama, Kanagawa 223-8522, Japan*

³*Faculty of Science and Technology, Keio University, Yokohama, Kanagawa 223-8522, Japan*

⁴*Department of Physics, The University of Tokyo, Tokyo 113-0033, Japan*

⁵*Institute for Solid State Physics, The University of Tokyo, Kashiwa 277-8581, Japan*



(Received 8 May 2024; accepted 10 June 2024; published 1 July 2024)

Efficient decomposition of multiqubit operators is critical in the execution of quantum algorithms. In this paper, we introduce decompositions of the multiple controlled-Z (CCZ and CCCZ) gates tailored to various qubit-coupling graphs. Specifically, we demonstrate that the CCZ gate is realized with CZ-depth 4 on a square-shaped qubit-coupling graph utilizing one auxiliary qubit. As for the CCCZ gate, previous research indicated that the decomposition requires 14 CZ gates in a fully connected topology. However, our findings reveal that only four specific qubit couplings are needed to achieve a decomposition using the same number of CZ gates, 14. Our research employs an optimization method to improve the alignment of parametrized quantum circuits with their intended quantum gates, which facilitates these efficient decompositions. This methodology is versatile and can be applied to decompose any quantum gates, not just the CCZ and CCCZ gates. These advancements in decomposing multiqubit gates, coupled with our CCZ and CCCZ decompositions, are poised to reduce quantum circuit execution times and enhance the efficiency of complex quantum algorithms in imminent quantum computing applications.

DOI: [10.1103/PhysRevA.110.012604](https://doi.org/10.1103/PhysRevA.110.012604)

I. INTRODUCTION

The efficient execution of complex qubit operations on a quantum processing unit (QPU) is a significant challenge in quantum computation, especially in today's quantum devices [1], where the total error correction is not yet available. When executing a given quantum circuit, the quantum compiler replaces all *high-level* multiqubit operations with sequences of *primitive* quantum gates that can be directly executed on the QPU. For example, recent trapped-ion QPUs have high connectivity, where we can perform two-qubit operations on arbitrary pairs of qubits [2,3]. On the other hand, superconducting QPUs generally have sparse couplings, and thus one can apply two-qubit gates only between limited pairs of qubits [4–6]. Given the variety of coupling graphs in different QPU technologies, it is crucial to develop novel decompositions for multiple controlled-Z (CCZ and CCCZ) gates that adapt to these different coupling constraints. This is particularly important when working with sparse couplings, where efficient decompositions can significantly improve the performance and feasibility of executing complex quantum operations.

The primitive gates supported by QPUs are usually one- and two-qubit gates. In principle, arbitrary multiqubit operations can be built as sequences of one- and two-qubit gates [7–9]. For example, Barenco *et al.* [10] and Cleve *et al.* [11]

have developed methods for building multiqubit controlled unitary operations. In the following, converting a multiqubit operation into a sequence of primitive gates is called the “decomposition.”

There are many studies on the decomposition of multiqubit operations, but they can be classified roughly according to whether they target fault-tolerant quantum computation or not.

In the context of fault-tolerant quantum computing, managing the computational cost associated with the T gates, which are single-qubit rotations by $\pi/4$ around the Z axis of the Bloch sphere, is crucial as they demand significant resources compared to the Clifford gates. This focus arises due to the fact that, in fault-tolerant implementations, the T -gate implementation is more complex and requires more overhead, particularly when quantum error correction schemes are employed. Therefore, in efforts to optimize quantum circuits for fault-tolerant applications, researchers prioritize minimizing the T count, the number of the T gates used, in the circuit design [12–21]. Jones [13] found an implementation of the Toffoli gate using four T gates. Gidney and Jones [14] found a decomposition of the CCCZ gate with six T gates. Various strategies to minimize the T depth have also been proposed [21–27]. Here, the T depth denotes the number of T stages involved in a computation, and a T stage is defined as a set of one or more T or T^\dagger gates that operate on distinct qubits and can be executed concurrently [22].


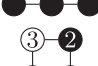
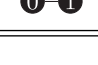
On the other hand, non-fault-tolerant quantum computing approaches do not emphasize heavily the cost of T gates. In these contexts, researchers generally focus more on the count or depth of two-qubit primitive gates to optimize performance

*Contact author: ken-nakanishi@g.ecc.u-tokyo.ac.jp

†Contact author: satoh@keio.jp

‡Contact author: wistaria@phys.s.u-tokyo.ac.jp

TABLE I. Decomposition of CCZ gate into CZ and one-qubit gates on various coupling graphs. The third one is the decomposition found in the present study. In the first column, the circles represent the qubits, the white circle represents the auxiliary qubit, and the lines represent the qubit couplings. The indices assigned to the qubits in the coupling graphs correspond to those in Fig. 1.


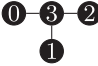
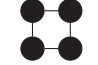
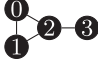

Coupling graph	CZ count	CZ depth	Reference
	6	6	Textbook implementation
	8	8	Gwinner <i>et al.</i> [46]
	8	4	Fig. 1

on near-term quantum devices, which are yet to implement full quantum error correction protocols [28–36]. A typical two-qubit gate in a quantum algorithm is the controlled-NOT (CNOT) gate, but not all QPUs can execute this operation directly. Available two-qubit elementary gates vary depending on the architecture of the QPU. Typical two-qubit elementary gates besides the CNOT gate are the iSWAP gate [37] and the CZ gate [38]. Schuch and Siewert [29] found decompositions of the CCCZ gate for several qubit-coupling graphs (Table II). Shende and Markov [31] determined that the minimum number of CZ gates, the *CZ count*, required to construct a CCCZ gate is 6.

In this paper, we discuss the decomposition of multiqubit operations for the non-fault-tolerant quantum computing approach. In the following, in addition to the CZ count, we also focus on the *CZ depth*, the number of *CZ stages* involved in a computation, where a *CZ stage* is defined as a set of one or more CZ gates that operate on distinct qubits and can be executed concurrently.

We have devised an optimization method for parametrized quantum circuits to find efficient decompositions of given multiqubit operations. There are many previous studies on the

TABLE II. Decomposition of CCCZ gate into CZ and one-qubit gates on various coupling graphs. The second and fourth are the decompositions found in the present study. In the first column, the circles represent the qubits, and the lines represent the qubit couplings. The indices assigned to the qubits in the coupling graphs correspond to those in Figs. 2 and 3.

Coupling graph	CZ count	CZ depth	Reference
	14	8	Schuch and Siewert [29]
	16	16	Nemkov <i>et al.</i> [47], Fig. 2
	16	8	Schuch and Siewert [29]
	14		Fig. 3
	18	12	Schuch and Siewert [29]

methods for finding the efficient decomposition of multiqubit operations [22,34,39–45]. In the present paper, we propose a method to search for the decomposition of multiqubit operations using a classical computer, taking moderate-sized qubit gates that fit the current classical computers as the targets. Several methods have been devised to decompose multiqubit operations by optimizing the rotation parameters in a parametrized quantum circuit. The steepest descent, the Broyden-Fletcher-Goldfarb-Shanno (BFGS) method, and simulated annealing methods have been used so far [39,41,44]. We have devised a technique that significantly reduces the computational complexity of the parameter optimization. Using this method, we can rapidly optimize the circuit parameters for a given parametrized quantum circuit to match the target quantum gate if possible. By examining various parametrized quantum circuits, we can find an efficient decomposition of the target multiqubit operations. It is also possible to replace the optimization part of the existing studies with our algorithm. Moreover, the proposed method can help us to check whether or not the already known decomposition of multiqubit operations is optimal.

We apply our optimization method to find decompositions of the CCZ and CCCZ gates on various qubit-coupling graphs. The CCZ and CCCZ gates are multi-qubit operations commonly used in quantum algorithms. As shown in Table II, efficient decompositions have been found for the CCZ and CCCZ gates on some graphs [28,29]. We found more decompositions on different graphs. We assume only the CZ gate is a two-qubit primitive gate. When the qubit-coupling graph is square-shaped and contains one auxiliary qubit, the CCZ gate can be decomposed with CZ-depth 4. The same applies to the Toffoli gate, which can be made with one CCZ and two one-qubit gates. The smallest number of CZ gates currently known to build a CCCZ gate is 14, which has been realized for the fully connected graph, which has six qubit couplings. We, however, found that this lower bound can be achieved using only four couplings between qubits. These decompositions are expected to shorten the execution time of quantum circuits and improve the accuracy of quantum algorithms on QPUs.

This paper is organized as follows: We present the efficient decompositions of the CCZ and CCCZ gates we found (Sec. II). Next, we describe the overall framework for searching for decompositions of multiqubit operations (Sec. III). Then, we explain the optimization method we used for finding optimal rotation angles of a parametrized quantum circuit (Sec. IV). Finally, we summarize the present study and give an outlook of future works (Sec. V).

II. MAIN RESULTS: DECOMPOSITIONS OF CCZ AND CCCZ GATES

To execute quantum algorithms on QPU efficiently and with high accuracy, we should reduce the execution time and the number of two-qubit operations.

The noise associated with the operations of a QPU arises cumulatively from the noise inherent in the primitive gates utilized in these operations. In real devices, two-qubit gates have smaller fidelities than one-qubit gates due to more noise involved in implementing the former. The two-qubit count

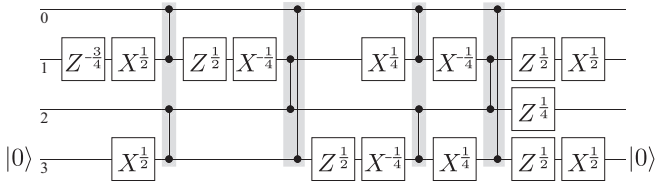


FIG. 1. Decomposition of the CCZ gate for a square-shaped qubit-coupling graph (third row in Table I). $X^a := R_X(a\pi)$, $Z^a := R_Z(a\pi)$. The CCZ gate can be decomposed with CZ-depth 4 (defined in Sec. II). The numbers assigned to each qubit correspond to the qubit indices in the coupling graph in Table I. The qubit at the bottom is used as an auxiliary qubit. Each gray zone represents a CZ stage, in which multiple CZ gates can be executed simultaneously.

after the decomposition should be as small as possible to reduce the noise.

To further reduce noise, it is crucial to minimize the execution time. For such a purpose, we consider the decomposition of multiqubit operations into as short a sequence of primitive gates as possible by assuming that qubit operations on nonoverlapping sets of qubits can be executed simultaneously. Significantly, the depth of two-qubit primitive gates, such as the CZ depth, is an essential metric for designing efficient decomposition [31].

Before going into the details of the methods, we present efficient decompositions of CCZ and CCCZ gates we found under different qubit-coupling graphs. These gates are typical three- and four-qubit gates. Here, we assume that the CZ gate is the only two-qubit primitive gate. Our main focus is on reducing the CZ count and/or the CZ depth of the decomposed multiqubit operations. Tables I and II summarize the decompositions of CCZ and CCCZ gates, respectively, for various qubit-coupling graphs. The decompositions we found are shown in Figs. 1–3.

III. SEARCH FOR DECOMPOSITIONS OF MULTIQUBIT OPERATIONS

This section describes the overall framework for searching for decompositions of multiqubit operations. In the following, we denote the X (Z) gate with rotation angle θ as $R_X(\theta)$ [$R_Z(\theta)$].

A. Parametrized quantum circuit generation

We start our search by determining the following: (1) type of two-qubit primitive gate to use, (2) QPU qubit-coupling

graph, and (3) initial two-qubit count or two-qubit depth of the circuit.

First, we enumerate all possible sequences of two-qubit primitive gates according to these conditions. Then, we insert parametrized one-qubit gates, more specifically, $R_Z(\theta)-R_X(\theta')-R_Z(\theta'')$, before and after each two-qubit primitive gate. [Especially when we consider the CZ gate as the two-qubit primitive gate, we can use $R_Z(\theta)-R_X(\theta')$ instead, except at the end of the circuit. This is because the CZ and R_Z gates commute with each other, and thus, omitting either one of the R_Z gates before or after the CZ gate does not spoil the representability of the parametrized circuit.] This way, we generate all the possible parametrized quantum circuits under the assumed conditions.

B. Exhaustive optimization of all prepared circuits

Next, we optimize rotation angles in the parametrized quantum circuits we prepared. Optimization details will be presented in Sec. IV. Since the optimization of rotation angles may stop at some local optimum, we repeat the optimization for each parametrized quantum circuit. The goal is achieved if the optimization finds a parametrized quantum circuit that matches the target quantum gate. Typically, a few optimization trials are enough to find the solutions, though more than one hundred trials are required for the CCCZ gates on the T-shaped coupling graph (the second row in Table II). We found that the CCCZ gate decomposition with 14 CZ gates can be achieved using only four couplings between qubits (the fourth row in Table II) instead of the fully connected graph. For the T-shaped qubit-coupling graph, we found a decomposition of the CCCZ gate with 16 CZ gates, which has the same CZ count as the one obtained by Nemkov *et al.* [47], but a different CZ-gate sequence. Our search for the T-shaped coupling graph case took about 37 h using a single NVIDIA GeForce RTX 4090. A detailed analysis of the efficiency of our method and theirs is subject to future work.

C. Further circuit simplification

Once optimal rotation angles are identified in a parametrized quantum circuit, we simplify the circuit by strategically reducing the number of single-qubit gates. This is achieved through extensive optimization, performing thousands to millions of iterations, each starting from random initial rotation angles. The goal is to converge on the target quantum gate configuration.

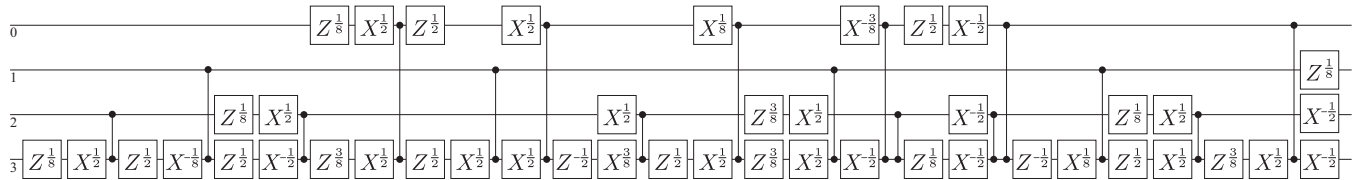


FIG. 2. Decomposition of CCCZ gate for a T-shaped qubit-coupling graph (second row in Table II). $X^a := R_X(a\pi)$, $Z^a := R_Z(a\pi)$. The CCCZ gate requires 16 CZ gates on the T-shaped qubit-coupling graph. The CZ count is the same as the decomposition obtained by Nemkov *et al.* [47], but the CZ-gate sequence is different. The numbers assigned to each qubit correspond to the qubit indices in the coupling graph in Table II.

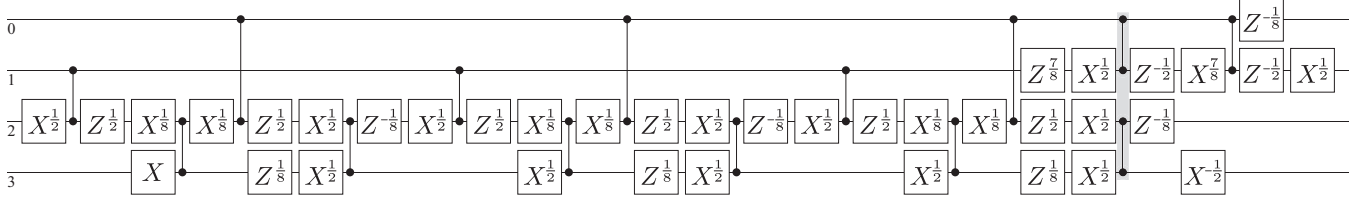


FIG. 3. Decomposition of CCCZ gate for qubit-coupling graph with only four couplings (fourth row in Table II). $X^a := R_X(a\pi)$, $Z^a := R_Z(a\pi)$. The smallest CZ count currently known is 14, which has been found for the fully connected graph. However, this lower bound can be achieved using only four couplings between qubits. The numbers assigned to each qubit correspond to the qubit indices in the coupling graph in Table II. Each gray zone represents a CZ stage, in which multiple CZ gates can be executed simultaneously.

After convergence, we analyze the distribution of each rotation angle. Any gate whose rotation angle converges frequently to zero or displays a near-uniform distribution can be eliminated by setting that angle to zero. This pruning process is repeated until no further reductions are feasible without compromising the circuit's functionality.

Subsequently, we refine the circuit by fixing the remaining nonzero rotation angles to simple rational multiples of π (e.g., $\pi/2$, $\pi/4$, $\pi/8$). This adjustment is iterated until all rotation angles stabilize at simple values, improving the circuit's efficiency and understandability.

IV. SEQUENTIAL OPTIMIZATION OF ROTATING GATES

In this section, we describe our sequential optimization algorithm for finding optimal rotation angles of a parametrized quantum circuit. While Nakanishi *et al.* [48] also employs a similar sequential optimization method, the calculation method for updating the parameters in the technique we propose is different. The two values required to update the parameters in our method are shown in Eqs. (14) and (15). Our method is also applicable to a circuit with auxiliary qubits. We design this algorithm to run on a classical computer. In Sec. IV A, we explain the property to be satisfied by the rotation gates in a parametrized quantum circuit and define the objective function Eq. (6). Then, in Sec. IV B, we explain the flow of the sequential optimization method to maximize the objective function Eq. (6).

A. Objective function

We assume that all rotation gates $R_A(\theta)$ in a parametrized quantum circuit are expressed as

$$R_A(\theta) = \exp\left(-\frac{i\theta}{2}A\right), \quad (1)$$

with A satisfying the following condition:

$$A^2 = I. \quad (2)$$

We also assume that the input quantum states are in the space spanned by D mutually orthogonal quantum states $\{|\Phi_d\rangle\}_{d=1}^D$, and P is defined as follows:

$$P := \sum_{d=1}^D |\Phi_d\rangle\langle\Phi_d|. \quad (3)$$

If the input space is the whole Hilbert space of the prepared c qubits, P is the 2^c -dimensional identity operator.

Let U_T be the target quantum gate we want to decompose, and U be a parametrized quantum circuit. The goal of the present algorithm is to optimize the parameters in U so that the output $\{U|\Phi_d\rangle\}_{d=1}^D$ becomes identical $\{U_T|\Phi_d\rangle\}_{d=1}^D$ except for the global phase common to all D states. This optimization problem is identical to finding U such that $f(U) = 0$ by minimizing $f(U)$ defined by

$$f(U) := \min_{\phi} \|e^{i\phi}U_T^\dagger U P - P\|_F^2, \quad (4)$$

where $\|\cdot\|_F$ denotes the Frobenius norm. Equation (4) can be transformed into the following equation:

$$f(U) = 2D - 2|\text{tr}[U_T^\dagger U P]|. \quad (5)$$

Thus, minimizing $f(U)$ until $f(U) = 0$ is equivalent to maximizing

$$|\text{tr}[U_T^\dagger U P]|^2 \quad (6)$$

until

$$|\text{tr}[U_T^\dagger U P]|^2 = D^2. \quad (7)$$

B. Rotation-angle optimization flow

Next, we describe how to optimize the parametrized quantum circuit sequentially. The optimization flow is shown in Fig. 4. Suppose that the parametrized quantum circuit U has K rotation gates. Then U can be written as

$$U(\theta_1, \dots, \theta_K) = V_K R_K(\theta_K) \cdots V_1 R_1(\theta_1) V_0, \quad (8)$$

where θ_k ($k = 1, \dots, K$) is the rotation angle of the k th rotation gate, and V_k ($k = 0, \dots, K$) denotes a fixed multiqubit unitary gate or an identity gate. Note that $V_k^{-1} = V_k$ ($k = 0, \dots, K$).

Let $U_n = U(\theta_1^{(n)}, \dots, \theta_K^{(n)})$ be the parametrized quantum circuit after n optimization steps. At the $(n+1)$ th step, first, we choose one of the rotation gates, say $R_k(\theta_k^{(n)})$, in the parametrized quantum circuit U_n . We rewrite the parametrized circuit U_n as

$$U_n = U_n' R_k(\theta_k^{(n)}) U_n'', \quad (9)$$

where

$$U_n' = V_K R_K(\theta_K^{(n)}) \cdots R_{k+1}(\theta_{k+1}^{(n)}) V_k, \quad (10)$$

$$U_n'' = V_{k-1} R_{k-1}(\theta_{k-1}^{(n)}) \cdots R_1(\theta_1^{(n)}) V_0. \quad (11)$$

Now we define $\tilde{U}_n(\theta)$ as

$$\tilde{U}_n(\theta) := U_n' R_k(\theta_k^{(n)} + \theta) U_n''. \quad (12)$$

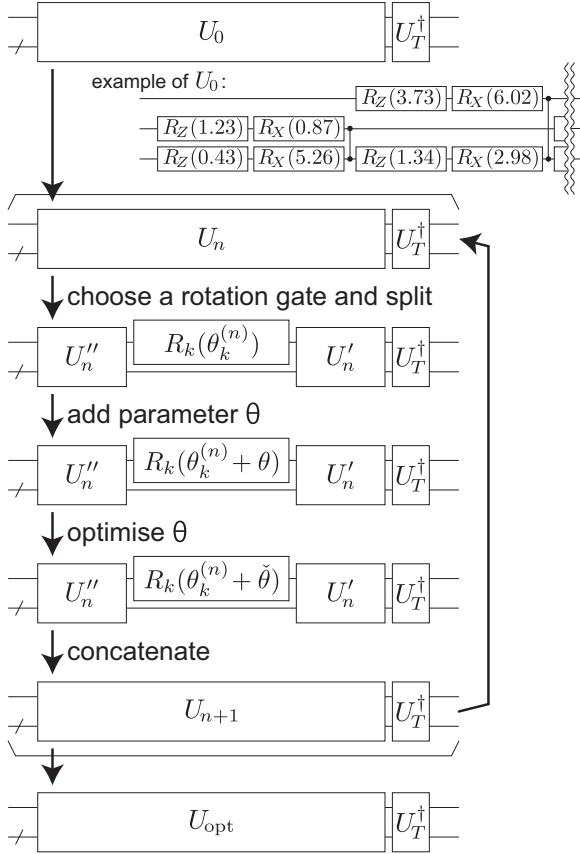


FIG. 4. Rotation-angle optimization flow. U_0 denotes the initial state of the parametrized quantum circuit, where the rotation angles are initialized uniformly randomly.

By using Eq. (12), the trace in Eq. (6) can be transformed as

$$\begin{aligned}
 & \text{tr}[U_T^\dagger \tilde{U}_n(\theta) P] \\
 &= \text{tr} \left[U_T^\dagger \tilde{U}_n(0) P \cos \frac{\theta}{2} + U_T^\dagger \tilde{U}_n(\pi) P \sin \frac{\theta}{2} \right] \\
 &= \text{tr}[U_T^\dagger \tilde{U}_n(0) P] \cos \frac{\theta}{2} + \text{tr}[U_T^\dagger \tilde{U}_n(\pi) P] \sin \frac{\theta}{2} \\
 &= t_0 \cos \frac{\theta}{2} + t_\pi \sin \frac{\theta}{2}, \tag{13}
 \end{aligned}$$

where

$$t_0 := \text{tr}[U_T^\dagger \tilde{U}_n(0) P] = \text{tr}[U_T^\dagger U_n P], \tag{14}$$

$$t_\pi := \text{tr}[U_T^\dagger \tilde{U}_n(\pi) P]. \tag{15}$$

By taking the square of the absolute value of Eq. (13), we finally obtain

$$\begin{aligned}
 & |\text{tr}[U_T^\dagger \tilde{U}_n(\theta) P]|^2 \\
 &= \left| t_0 \cos \frac{\theta}{2} + t_\pi \sin \frac{\theta}{2} \right|^2 \\
 &= |t_0|^2 \cos^2 \frac{\theta}{2} + |t_\pi|^2 \sin^2 \frac{\theta}{2} + (t_0 t_\pi^* + t_0^* t_\pi) \cos \frac{\theta}{2} \sin \frac{\theta}{2} \\
 &= \frac{|t_0|^2 - |t_\pi|^2}{2} \cos \theta + \frac{t_0 t_\pi^* + t_0^* t_\pi}{2} \sin \theta + \frac{|t_0|^2 + |t_\pi|^2}{2}, \tag{16}
 \end{aligned}$$

where t^* denotes the complex conjugate of t . From Eq. (16), we can find $\check{\theta}$ that maximizes $|\text{tr}[U_T^\dagger \tilde{U}_n(\theta) P]|^2$ as

$$\begin{aligned}
 \check{\theta} &:= \arg \max_\theta (|\text{tr}[U_T^\dagger \tilde{U}_n(\theta) P]|^2) \\
 &= \begin{cases} \arctan \left(\frac{t_0 t_\pi^* + t_0^* t_\pi}{|t_0|^2 - |t_\pi|^2} \right), & |t_0|^2 - |t_\pi|^2 > 0, \\ \arctan \left(\frac{t_0 t_\pi^* + t_0^* t_\pi}{|t_0|^2 - |t_\pi|^2} \right) + \pi, & |t_0|^2 - |t_\pi|^2 < 0, \end{cases} \tag{17}
 \end{aligned}$$

which defines U_{n+1} for the next iteration:

$$U_{n+1} := \tilde{U}_n(\check{\theta}). \tag{18}$$

In other words, without having to calculate the gradient, local optimization for θ can be performed just by calculating the two values, t_0 and t_π .

From Eqs. (14), (16), and (18), the following inequality can be derived,

$$|\text{tr}[U_T^\dagger U_{n+1} P]|^2 \geq |\text{tr}[U_T^\dagger U_n P]|^2, \tag{19}$$

that is, the objective function (6) increases monotonically as the optimization proceeds. By updating each rotation gate $R_k(\theta_k)$ ($k = 1, \dots, K$) sequentially according to the above procedure, we can optimize U so that $|\text{tr}[U_T^\dagger U P]|^2$ is maximized. If $|\text{tr}[U_T^\dagger U P]|^2$ is maximized until D^2 , the parametrized quantum circuit becomes identical to the target quantum gate, meaning that we successfully find a decomposition of U_T .

C. Reduction of computation complexity

To reduce the computation complexity, we can exploit the cyclic property of the trace. In the objective function at the $(n+1)$ step, we can bring the chosen rotation gate to the leftmost as

$$|\text{tr}[U_T^\dagger \tilde{U}_n(\theta) P]|^2 = |\text{tr}[R_k(\theta_k^{(n)} + \theta) M_n]|^2, \tag{20}$$

where

$$M_n = U_n'' P U_T^\dagger U_n'. \tag{21}$$

If we choose $R_{k-1}(\theta_{k-1})$ or $R_{k+1}(\theta_{k+1})$ as the target rotation gate of the next step, M_{n+1} can be easily calculated as

$$M_{n+1} = R_{k-1}(-\theta_{k-1}^{(n)}) V_{k-1} M_n R_k(\check{\theta}) V_{k-1} \tag{22}$$

or

$$M_{n+1} = V_k R_k(\check{\theta}) M_n V_k R_{k+1}(-\theta_{k+1}^{(n)}), \tag{23}$$

respectively, by using the following properties: $R_k^{-1}(\theta_k) = R_k(-\theta_k)$ and $V_k^{-1} = V_k$. In the present calculation, we choose the rotation gates in the following order:

$$\begin{aligned}
 & K \rightarrow K-1 \rightarrow \dots \rightarrow 2 \rightarrow 1 \rightarrow 2 \rightarrow \dots \rightarrow K-1 \rightarrow K \\
 & \rightarrow K-1 \rightarrow \dots .
 \end{aligned}$$

Using this technique, we can reduce the computational cost significantly compared to calculating U_n from scratch at each optimization step.

V. CONCLUSION

In the present paper, we presented efficient decompositions of the CCZ and CCCZ gates under various qubit-coupling

graphs. The CCZ and CCCZ gates are multiqubit gates commonly used in quantum circuits. We can achieve more efficient and less error-prone quantum circuits using these decompositions, especially for QPUs with sparse coupling graphs, such as the superconducting QPUs.

Contributing to this finding is our sequential optimization algorithm of a parametrized quantum circuit. By using our method, we can optimize the rotation angles for a given parametrized quantum circuit to achieve the target quantum gate. The present optimization method can be used not only for the CCZ and CCCZ gates but also for arbitrary qubit gates. Since the method does not depend on any particular primitive gate set, it can be modified and applied to various QPUs. Using this method to find a suitable decomposition of multiqubit operations for particular QPUs will reduce the execution time of quantum circuits on QPUs and improve the accuracy of quantum algorithms. It is also possible to replace the parameter optimization part of the existing decomposition research with this method. We believe that the present optimization method will be an essential tool for error reduction. Not

only that, but the analysis of the decomposition of multiqubit operations found in the present study may provide hints for designing larger-scale multiqubit gates in the future.

ACKNOWLEDGMENTS

This calculation has been done using NVIDIA GPGPU at the Institute for Physics of Intelligence ($i\pi$), School of Science, the University of Tokyo. K.M.N. has been supported by KAKENHI No. 20J13955 and is supported by the Daikin Endowed Research Unit: “Research on Physics of Intelligence,” School of Science, the University of Tokyo. T.S. is supported by MEXT Quantum Leap Flagship Program Grants No. JPMXS0118067285 and No. JPMXS0120319794, JST Grant No. JPMJPF2221, and MEXT KAKENHI Grant No. 22K1978. S.T. acknowledges support by the Endowed Project for Quantum Software Research and Education, The University of Tokyo [49] and the Center of Innovations for Sustainable Quantum AI [50] (JST Grant No. JPMJPF2221).

-
- [1] J. Preskill, *Quantum* **2**, 79 (2018).
- [2] K. Wright, K. Beck, S. Debnath, J. Amini, Y. Nam, N. Grzesiak, J.-S. Chen, N. Plesch, M. Chmielewski, C. Collins *et al.*, *Nat. Commun.* **10**, 1 (2019).
- [3] B. Yirka, Honeywell claims to have built the highest-performing quantum computer available, <https://phys.org/news/2020-06-honeywell-built-highest-performing-quantum.html> (2020).
- [4] J. Kelly, A preview of bristlecone, Google’s new quantum processor, <https://research.google/blog/a-preview-of-bristlecone-googles-new-quantum-processor/>.
- [5] IBM, IBM announces advances to IBM quantum systems & ecosystem, <https://www-03.ibm.com/press/us/en/pressrelease/53374.wss> (2017).
- [6] S. Caldwell, N. Didier, C. Ryan, E. Sete, A. Hudson, P. Karalekas, R. Manenti, M. da Silva, R. Sinclair, E. Acala *et al.*, *Phys. Rev. Appl.* **10**, 034050 (2018).
- [7] D. Deutsch, A. Barenco, and A. Ekert, *Proc. R. Soc. Lond. A* **449**, 669 (1995).
- [8] S. Lloyd, *Phys. Rev. Lett.* **75**, 346 (1995).
- [9] M. J. Bremner, C. M. Dawson, J. L. Dodd, A. Gilchrist, A. W. Harrow, D. Mortimer, M. A. Nielsen, and T. J. Osborne, *Phys. Rev. Lett.* **89**, 247902 (2002).
- [10] A. Barenco, C. H. Bennett, R. Cleve, D. P. DiVincenzo, N. Margolus, P. Shor, T. Sleator, J. A. Smolin, and H. Weinfurter, *Phys. Rev. A* **52**, 3457 (1995).
- [11] R. Cleve, A. Ekert, C. Macchiavello, and M. Mosca, *Proc. R. Soc. London, Ser. A* **454**, 339 (1998).
- [12] P. Selinger, *Phys. Rev. A* **87**, 042302 (2013).
- [13] C. Jones, *Phys. Rev. A* **87**, 022328 (2013).
- [14] C. Gidney and N. C. Jones, [arXiv:2106.11513](https://arxiv.org/abs/2106.11513).
- [15] J. Jiang and X. Wang, *Phys. Rev. Appl.* **19**, 034052 (2023).
- [16] N. de Beaudrap, X. Bian, and Q. Wang, [arXiv:2004.05164](https://arxiv.org/abs/2004.05164).
- [17] V. Kliuchnikov, D. Maslov, and M. Mosca, *IEEE Trans. Comput.* **65**, 161 (2016).
- [18] N. J. Ross and P. Selinger, *Quantum Inf. Comput.* **16**, 901 (2016).
- [19] D. Gosset, V. Kliuchnikov, M. Mosca, and V. Russo, *Quantum Inf. Comput.* **14**, 1261 (2014).
- [20] M. Mosca and P. Mukhopadhyay, *Quantum Sci. Technol.* **7**, 015003 (2022).
- [21] V. Gheorghiu, M. Mosca, and P. Mukhopadhyay, *npj Quantum Inf.* **8**, 141 (2022).
- [22] M. Amy, D. Maslov, M. Mosca, and M. Roetteler, *IEEE Trans. Comput.-Aided Design Integr. Circuits Syst.* **32**, 818 (2013).
- [23] M. Amy, D. Maslov, and M. Mosca, *IEEE Trans. Comput.-Aided Design Integr. Circuits Syst.* **33**, 1476 (2014).
- [24] V. Gheorghiu, M. Mosca, and P. Mukhopadhyay, *npj Quantum Inf.* **8**, 110 (2022).
- [25] P. Niemann, A. Gupta, and R. Drechsler, in *2019 IEEE 49th International Symposium on Multiple-Valued Logic (ISMVL)* (IEEE, New York, 2019), pp. 108–113.
- [26] J. Lee, S. Lee, Y.-S. Lee, and D. Choi, *IET Information Security* **17**, 46 (2023).
- [27] Z. Huang and S. Sun, in *International Conference on the Theory and Application of Cryptology and Information Security* (Springer, Berlin, 2022), pp. 614–644.
- [28] N. Schuch and J. Siewert, *Phys. Rev. Lett.* **91**, 027902 (2003).
- [29] N. Schuch and J. Siewert, Implementation of quantum algorithms with Josephson charge qubits, Ph.D. thesis, Universität Regensburg, 2002.
- [30] M. Möttönen, J. J. Vartiainen, V. Bergholm, and M. M. Salomaa, *Phys. Rev. Lett.* **93**, 130502 (2004).
- [31] V. V. Shende and I. L. Markov, *Quantum Inf. Comput.* **9**, 461 (2009).
- [32] B. Park and D. Ahn, *Sci. Rep.* **13**, 8638 (2023).
- [33] T. G. d. Brugière, M. Baboulin, B. Valiron, S. Martiel, and C. Allouche, *IEEE Trans. Quantum Eng.* **2**, 1 (2021).
- [34] D. Maslov, *Phys. Rev. A* **93**, 022311 (2016).
- [35] X. Liu, H. Yang, and L. Yang, *Secur. Commun. Netw.* **1**, 2963110 (2023).

- [36] X. Liu, H. Yang, and L. Yang, *Cybersecurity* **6**, 48 (2023).
- [37] X. Y. Han, T. Q. Cai, X. G. Li, Y. K. Wu, Y. W. Ma, Y. L. Ma, J. H. Wang, H. Y. Zhang, Y. P. Song, and L. M. Duan, *Phys. Rev. A* **102**, 022619 (2020).
- [38] J. Ghosh, A. Galiatdinov, Z. Zhou, A. N. Korotkov, J. M. Martinis, and M. R. Geller, *Phys. Rev. A* **87**, 022309 (2013).
- [39] S. Khatri, R. LaRose, A. Poremba, L. Cincio, A. T. Sornborger, and P. J. Coles, *Quantum* **3**, 140 (2019).
- [40] D. Venturelli, M. Do, E. Rieffel, and J. Frank, *Quantum Sci. Technol.* **3**, 025004 (2018).
- [41] L. Cincio, Y. Subaşı, A. T. Sornborger, and P. J. Coles, *New J. Phys.* **20**, 113022 (2018).
- [42] E. Zahedinejad, J. Ghosh, and B. C. Sanders, *Phys. Rev. Appl.* **6**, 054005 (2016).
- [43] K. E. Booth, M. Do, J. C. Beck, E. Rieffel, D. Venturelli, and J. Frank, in *Twenty-Eighth International Conference on Automated Planning and Scheduling* (Association for the Advancement of Artificial Intelligence, 2018), pp. 366–374.
- [44] E. A. Martinez, T. Monz, D. Nigg, P. Schindler, and R. Blatt, *New J. Phys.* **18**, 063029 (2016).
- [45] E. Younis, K. Sen, K. Yelick, and C. Iancu, [arXiv:2003.04462](https://arxiv.org/abs/2003.04462).
- [46] J. Gwinner, M. Briański, W. Burkot, Ł. Czerwiński, and V. Hlembotskyi, [arXiv:2007.06539](https://arxiv.org/abs/2007.06539).
- [47] N. A. Nemkov, E. O. Kiktenko, I. A. Luchnikov, and A. K. Fedorov, *Quantum* **7**, 993 (2023).
- [48] K. M. Nakanishi, K. Fujii, and S. Todo, *Phys. Rev. Res.* **2**, 043158 (2020).
- [49] <https://qsw.phys.s.u-tokyo.ac.jp/>
- [50] <https://sqai.jp/>